Chemical Geology 420 (2016) 200–212

Contents lists available at ScienceDirect

Chemical Geology

journal homepage: www.elsevier.com/locate/chemgeo

Seasonal variability in concentrations and fluxes of glycerol dialkyl glycerol tetraethers in Huguangyan Maar Lake, SE China: Implications for the applicability of the MBT–CBT paleotemperature proxy in lacustrine settings

Jianfang Hu [a,*], Haoda Zhou [a,b], Ping'an Peng [a], Baruch Spiro [c]

[a] State Key Laboratory of Organic Geochemistry, Guangzhou Institute of Geochemistry, Chinese Academy of Sciences, Guangzhou, 510640, PR China
[b] Zhuhai Central Station of Marine Environmental Monitoring, State Oceanic Administration, Zhuhai 519015, PR China
[c] Department of Mineralogy, The Natural History Museum, Cromwell Road, London SW7 5BD, UK

ARTICLE INFO

Article history:
Received 22 May 2015
Received in revised form 7 November 2015
Accepted 11 November 2015
Available online 1 December 2015

Keywords:
Subtropical South China
Maar lake
Branched GDGTs
MBT–CBT proxy
Palaeoclimate

ABSTRACT

Glycerol dialkyl glycerol tetraethers (GDGTs) are increasingly used for paleoclimate studies of marine and lacustrine environments. Although GDGT-based proxies have been applied to various lake environments globally, little is known about the distribution of GDGTs in lakes in subtropical South China, which are mainly controlled by the East Asian monsoonal system. Therefore, we investigated the distribution of GDGTs in Huguangyan Maar Lake (HML) in order to examine their characteristics as paleoclimate proxies in subtropical South China. Suspended particulate matter (SPM) in the water column was sampled monthly over a one year period at three different depths. Sediment traps were deployed simultaneously at the same locations and settling particles were collected monthly over a one year period too. In order to identify the sources of GDGTs in HML, lake bottom sediments and soil samples from the catchment were collected. The distribution and abundance of GDGTs in all samples were determined and GDGT-based temperatures were calculated.

The concentrations and fluxes of GDGTs of settling particles in HML were dominated by branched GDGTs, with a minor contribution of isoprenoid homologues. The maximum concentrations and fluxes of branched GDGTs occurred during the winter months, when the water column was well mixed due to the strong East Asian winter monsoon. Also, maximal concentrations and fluxes of branched GDGTs were observed at the deeper water mass. These observations suggest that *in situ* production of branched GDGTs takes place mainly in the deeper part of the water column and/or at the sediment–water interface, but may be influenced by seasonal variability in the primary production in the shallower water mass of HML. The temperatures calculated from the methylation of branched tetraethers (MBT) and the cyclization ratio of branched tetraethers (CBT) of SPM and settling particles were lower than local air temperature (AT) during spring and summer when the water column was in thermal stratification, and were higher than AT during fall and winter when the water column was isothermal. However, the MBT–CBT based temperatures were in good agreement with AT on an annual time scale. Therefore they can be used as a proxy of local air temperature. Furthermore, the variations in concentration and flux of GDGTs are synchronous with the East Asian monsoon annual cycle. The overall amplitude of the estimated monthly temperature is however smaller than that of the measured air temperature. The mean MBT–CBT based temperature estimates (23.4 ± 0.6 °C) of lake bottom sediments for that one year period agree with the local average mean air temperature (23.1 ± 0.5 °C) for the preceding 45 years, providing further support to the reliability of this proxy and the interpretation of the results. Both long term stratification and mixing events in water column might present a challenge to the application of branched GDGT-based paleoenvironmental proxies in lakes. The present study reveals that GDGTs in lakes within the area influenced by the East Asian monsoon have a considerable potential for paleoclimatic studies but it is important to determine the location and nature of the sources of GDGTs sampled in lacustrine environments prior to their interpretation as paleoclimatic indicators. More generally, this study identifies factors which have to be considered in order to obtain reliable palaeotemperature data from GDGTs in lacustrine settings.

1. Introduction

Recently, organic proxies based on the relative abundance of microbial membrane lipids i.e., glycerol dialkyl glycerol tetraethers (GDGTs)

* Corresponding author.
E-mail address: hujf@gig.ac.cn (J. Hu).

http://dx.doi.org/10.1016/j.chemgeo.2015.11.008
0009-2541/

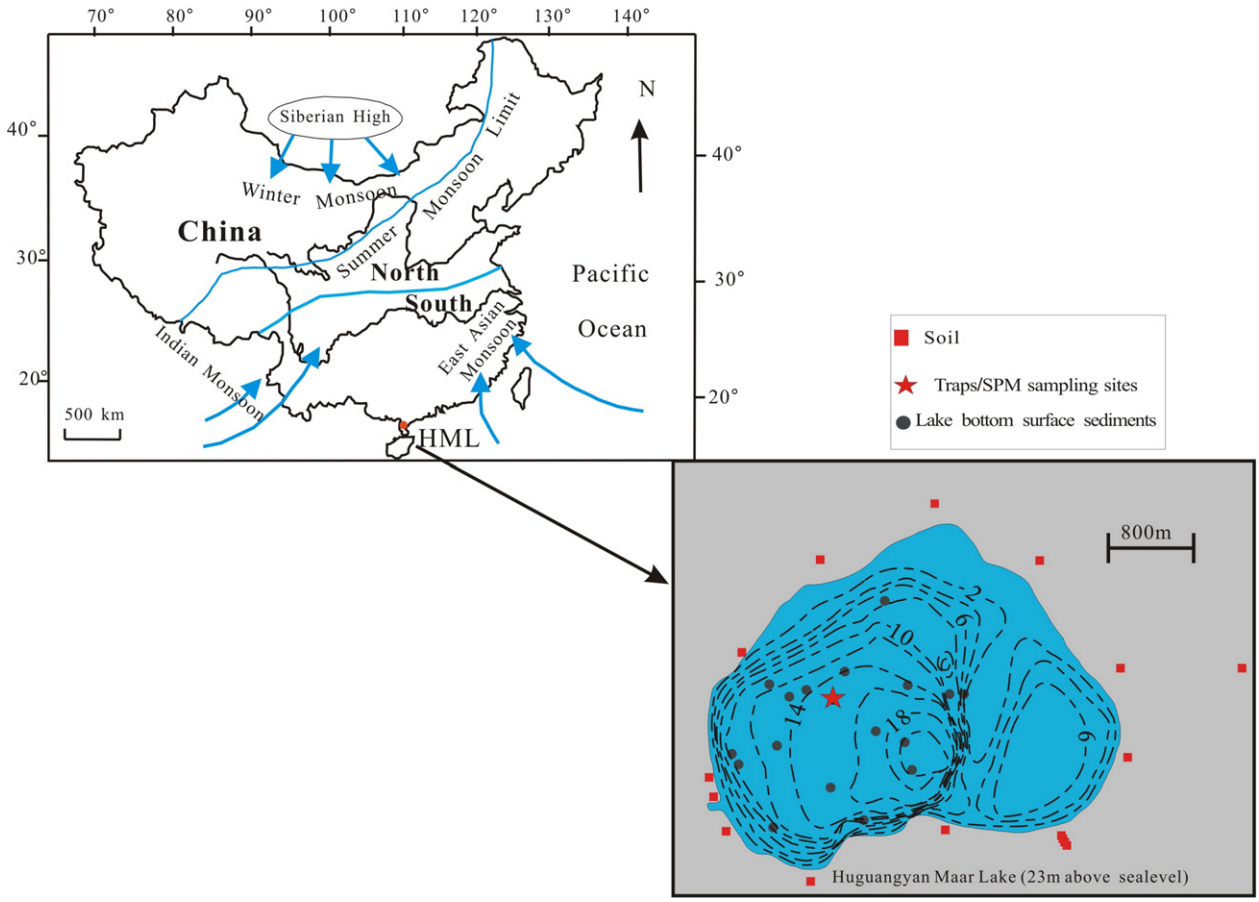

Fig. 1. A map showing the location of Huguangyan Maar Lake (HML) and the monsoonal system in China. The sampling sites for soil, surface sediments, suspended particulate matter (SPM) and sediment traps are shown in the inserted map. The contours indicate water depth (m).

were developed to reconstruct historical temperature records of lake water and continental air temperatures (e.g. Powers et al., 2005; Tierney et al., 2008, 2010a,b). GDGTs have a strong potential as paleotemperature proxies in lakes, as the relative distribution of isoprenoid GDGTs and also branched GDGTs was found to be temperature dependent (Schouten et al., 2002; Weijers et al., 2007a). One such proxy is TEX_{86} (TetraEther indeX of tetraethers consisting of 86 carbon atoms; Schouten et al., 2002), which has been successfully used in studies of long term, high-resolution temperature records of several lakes in the East African Rift (Powers et al., 2005; Tierney et al., 2008; Woltering et al., 2011). However, TEX_{86} was found to be useful only in large lakes with high proportions of isoprenoidal to branched GDGTs (Blaga et al., 2009; Powers et al., 2010). Hopmans et al. (2004) quantified the abundance of branched GDGTs relative to that of isoprenoid GDGTs in aquatic systems, expressed as the branched versus isoprenoid tetraether (BIT) index. This was then used as a measure of the relative inputs of soil organic matter and the *in situ* produced aquatic contribution to the total organic matter found in lake sediments (Hopmans et al., 2004; Weijers et al., 2007a; Walsh et al., 2008).

Another proxy proposed for the reconstruction of past annual mean air temperature (MAT; Weijers et al., 2007b) is based on branched GDGTs in soils. Two indices were developed based on the relative abundance of different branched GDGTs, i.e. the MBT (Methylation index of Branched Tetraethers), which correlate with MAT and to a lesser extent with soil pH, and the CBT (Cyclization ratio of Branched Tetraethers), which depend on soil pH (Weijers et al., 2007b). Recent studies have shown that MBT and CBT are significantly correlated with MAT in lakes, for example in East Africa (Tierney et al., 2010b) and New Zealand (Zink et al., 2010). These findings highlight the potential for branched GDGTs to be used as a paleothermometer in a large variety of lacustrine settings. However, application of this proxy in lakes may be complicated by in situ production of branched GDGTs in the water column and/or the sediment (e.g. Tierney and Russell, 2009; Tierney et al., 2010b; Sun et al., 2011; Loomis et al., 2011, Schouten et al., 2013). Furthermore, MBT–CBT reconstructed temperatures from different lacustrine settings may be biased by factors such as seasonality of primary production and/or preferred depth habitat of the related microorganisms (Sun et al., 2011).

Many uncertainties currently exist regarding sources of branched GDGTs found in lakes, and thus the use of MBT–CBT as a paleothermometer of lakes (review by Schouten et al., 2013). Despite the fact that *in-situ* production of branched GDGTs likely occurs in variable proportions in different lakes, several studies suggest that it is still possible to reconstruct MAT using the MBT–CBT proxies (e.g. Zink et al., 2010; Fawcett et al., 2011; Sun et al., 2011; Loomis et al., 2012; Naeher et al., 2014). In order to further improve the reliability of GDGT-based proxies in lakes, it is necessary to better understand the sources of the GDGTs in lacustrine systems. Furthermore, it is necessary to address the issue of seasonality of the GDGT-based proxies in lakes.

The Huguangyan Maar Lake (HML) is situated at the confluence of the East Asian monsoon, which is influenced by the climate regime of northern cold fronts originating from the Siberian anti-cyclone with the Southwest Asian summer monsoon from the Indian Ocean and the Southeast summer monsoon from the Pacific Ocean (Yancheva et al., 2007; Wu et al., 2012). Its geographical, geomorphological and hydrological features, and high-resolution well bedded sediments have a great potential for the investigation of the evolution of Asian monsoon (Fuhrmann et al., 2003; Mingram et al., 2004; Wang et al., 2007; Yancheva et al., 2007; Wu et al., 2012) in the subtropical South China. For this region therefore, the development of new proxies and the

integration of multiple independent approaches for reliable continental temperature estimates are of great importance.

Therefore, this study aims to: 1) investigate the vertical distribution and seasonal variation of GDGTs in the water column of HML as a representative of subtropical South China, 2) identify their sources and determine their respective pathways and 3) carry out appropriate calibrations for estimating local air temperature based on the lake bottom sediments and records of mean annual air temperatures. Furthermore, the study aims to improve the basis for the application of GDGT-derived parameters and their interpretation as records of paleotemperature in subtropical South China, and hence lacustrine sediments in similar environmental settings.

2. Material and methods

2.1. Geographical setting

Huguangyan Maar Lake (HML) (21°9′N, 110°17′E) is a closed maar lake, within a crater basin created by basaltic phreatomagmatic eruptions (Liu, 1999). The tephra ring rises 10–58 m above the lake surface and consists of pyroclastic sediments (Chu et al., 2002). It is located in the Zhanjiang area, on the low-lying Leizhou Peninsula in the southernmost part of the Chinese mainland (Fig. 1). The fresh water lake (~23 m above sea level) has a surface area of 2.3 km^2 and a maximum depth of 20 m. Its catchment area (3.5 km^2) comprises only the inner slopes of the crater rim. The lake has no surface inflow or outflow (Chu et al., 2002), with the thermocline fluctuating between 6 and 13 m depth.

The HML is located within an area of subtropical climate controlled by the East Asian monsoon. It is influenced by the winter monsoon, northern cold fronts originating from the Siberian anti-cyclone, the Asian Southwest summer monsoon from the Indian Ocean and Southeast summer monsoon from the West Pacific Ocean. During winter, the strong East Asian winter monsoon with northeasterly winds blowing over HML causes the mixing of the HML water. By contrast, during summer, the lake is strongly stratified due to high air temperatures and weak winds (Wang et al., 2008, 2012). When the summer monsoon is strong, the climate in Zhanjiang area is wet and the lake level is high (Wu et al., 2012). The climate in this area is highly seasonal, with 90% of the total mean annual precipitation of 1567 mm falling between April and October (Chu et al., 2002), while the cold and dry season lasts from November to March. The average value of the MAT in Zhanjiang (15 km from HML) over the last 45 years has been 23.1 °C (Mingram et al., 2004). The average temperature in the hottest month (July) is 29 °C and in the coldest (January) is 18 °C. The lowest temperature 3.8 °C was recorded in 1955 (Zheng and Lei, 1999). In biogeographical terms the lake belongs to a zone of subtropical grassland, and the natural vegetation is that of a tropical semi-evergreen seasonal rain forest (Zheng and Lei, 1999).

2.2. Sample collection

Sampling of suspended particulate matter (SPM) was performed monthly at the middle of each month of the 13-month period starting in October 2011 and ending in October 2012. This was carried out from a boat, along a vertical profile in the center of the lake (Fig. 1). Samples were taken on board the boat at 0.5, 6.5, and 16 m water depth from 8 am to 4 pm. On the same days sediment traps used for the collection of settling particles, were recovered and redeployed. Water column temperature profiles were obtained at depths of 0.5, 6.5, and 16 m, using mini CTD profilers (Valeport, Devon, UK) accuracy is ±0.3 °C, at a 1.5 h interval during the same monthly SPM and sediment trap sampling, from November 2011 to October 2012. The pH values of waters were measured during the same time as sampling and temperature measurements.

SPM samples were separated from water samples (20–30 L) collected with 8 L Niskin bottles using an in situ filtration system equipped with 142 mm diameter pre-combusted 0.7 μm nominal pore size Whatman GF/F filters. After filtration, the filters were stored at −20 °C and freeze-dried in the laboratory.

The settling particles were collected in twelve open cylinder sediment traps (height 50 cm, ø 11.0 cm) with four traps at each of the three water depths (0.5, 6.5, and 16 m). The traps were not poisoned, but the relatively short time (i.e., 4 weeks maximum) between deployment and sampling was thought to be short enough so that no substantial alteration of the GDGTs occurred during the time of deployment (Blaga et al., 2011). The first sediment traps were deployed at the end of September 2011 and were recovered in November 2011. After the sediment traps were recovered, the overlying water layer was drained and samples were centrifuged at 6000 rpm for 20 min. The separated particulate matter was then kept at −20 °C and freeze-dried in the laboratory. Particulate matter was weighed after freeze-drying to calculate particle fluxes ($g \cdot m^{-2} \cdot d^{-1}$).

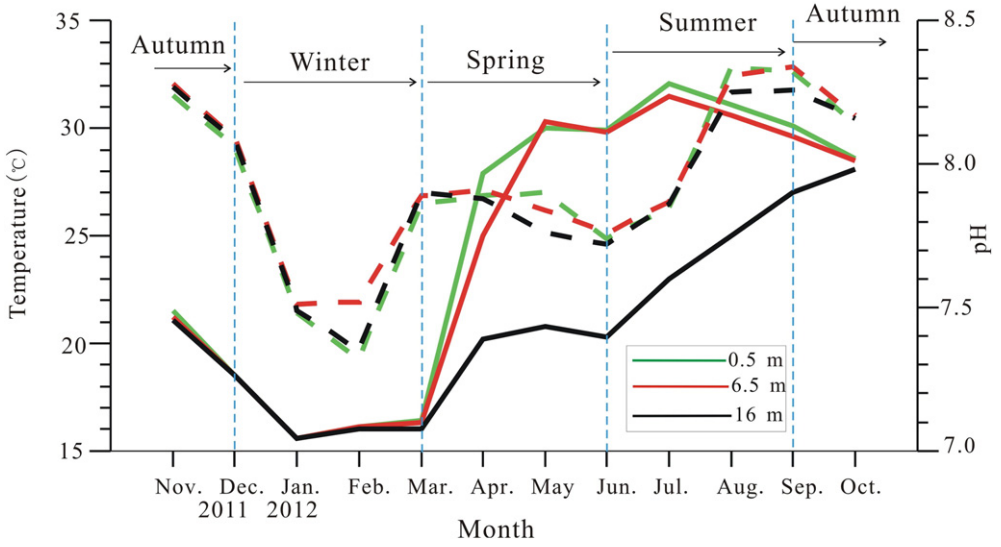

Fig. 2. Profiles of temperature (solid line) and pH (dotted line) from three sampling depths (0.5 m, 6.5 m and 16 m depth) in the water column of Huguangyan Maar Lake from November 2011 to October 2012. The profiles show that the water column was nearly isothermal – well mixed during the winter – the effect of the winter monsoon, and that thermal stratification began in March and ended in late October. The pH values were higher in winter.

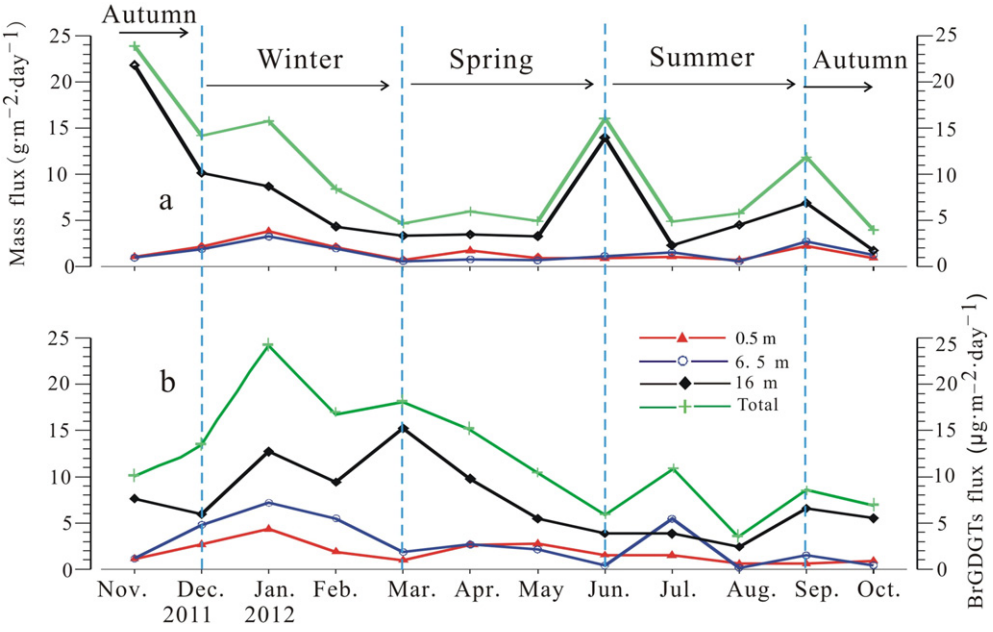

Fig. 3. Annual mass flux variations in Huguangyan Maar Lake of a) settling particles and b) branched GDGTs collected in sediment traps at 0.5 m, 6.5 m and 16 m water depth from November 2011 to October 2012. The fluxes of total particulate matter mass and branched GDGTs were higher in winter than in other seasons.

In order to better identify the sources of GDGTs in HML (autochthonous vs. allochthonous), 17 samples of lake bottom sediment (0–3 cm) were collected using a stainless steel box corer. Among them, 6 samples were collected on March 13, 2010; the other 11 samples were collected in November 2011. In addition, 4 samples of top soil (0–10 cm) from locations around the lake were collected in March 2010 and 12 samples of top soil from locations around the lake were collected in March 2012 for examination of GDGTs and comparison with those of the HML (Fig. 1). At each site, soils were sampled in triplicate and mixed to account for heterogeneity. All of the soil samples were collected using a clean stainless steel shovel, and all collected samples were wrapped in solvent-cleaned aluminum foil and stored at −20 °C until analysis.

2.3. GDGT analysis

Soils and sediments were freeze-dried, ground into fine powder, and spiked with an appropriate amount of C_{46}-GDGT (standard compound). Then, 5–15 g of the powdered samples was extracted with an azeotropic

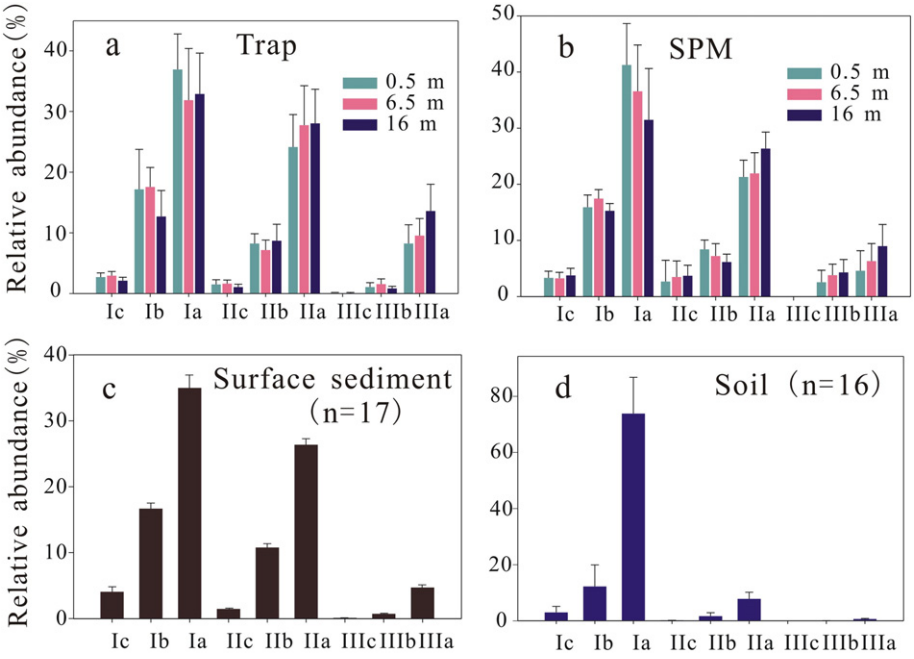

Fig. 4. Histogram of the average relative abundance of nine branched GDGTs (for structure see Appendix A) in the Huguangyan Maar Lake from a) traps and b) suspended particulate matter at three different water depths during the monitoring period from November 2011 to October 2012, as well as from c) lake bottom surface sediments (n = 17) and d) catchment soils (n = 16). The histograms show that the molecular distribution of branched GDGTs in traps, SPM, and surface sediments of HML was identical, but catchment area was different.

mixture of dichloromethane/methanol (2/1, v/v) in a Soxhlet apparatus for 72 h. The freeze-dried GF/F filters containing SPM and a weighed aliquot of freeze-dried settling particulate matter were extracted stepwise in an ultrasonic bath along a gradient from 100% methanol to 100% DCM; and a total of nine extraction steps. All extracts were rotary evaporated to dryness and re-dissolved in a small amount of hexane/DCM (9:1, v/v). The extracts were fractionated by column chromatography on neutral alumina. The apolar and polar fractions were eluted with hexane/DCM (9:1, v:v) and DCM/methanol (1:1, v:v), respectively. The polar fraction (DCM/methanol) was recovered by rotary evaporation, dissolved in hexane/isopropanol (99:1, v/v), and filtered through a 0.45 μm polytetrafluoroethene filter prior to analysis.

High-performance liquid chromatography/atmospheric pressure chemical ionization-mass spectrometry (HPLC/APCI-MS) was used to analyze the GDGT content of all samples. Analyses were performed using an Agilent 1200 series liquid chromatograph equipped with an auto-injector and ChemStation chromatography management software. The conditions for HPLC/APCI-MS were set as stated in Zhou et al. (2014). GDGTs were detected by using selected ion monitoring (SIM) mode following the methods described by Schouten et al. (2007). Quantification was achieved by integration of the peak area of $[M + H]^+$ ion traces of GDGTs. Each sample was analyzed in duplicate and the data presented are mean values. Absolute amounts of GDGTs were calculated following Huguet et al. (2006). Replicate HPLC/APCI-MS analysis of one sample revealed the reproducibility of the BIT index, CBT, and MBT to be ±0.036, ± 0.010, and ±0.010, respectively. Indices based on the distribution of GDGTs were calculated as follows (Hopmans et al., 2004; Weijers et al., 2007b):

$$\mathrm{BIT} = \frac{\mathrm{Ia} + \mathrm{IIa} + \mathrm{IIIa}}{\mathrm{Ia} + \mathrm{IIa} + \mathrm{IIIa} + \mathrm{Cren.}}$$

$$\mathrm{MBT} = \frac{\mathrm{Ia} + \mathrm{Ib} + \mathrm{Ic}}{(\mathrm{Ia} + \mathrm{Ib} + \mathrm{Ic}) + (\mathrm{IIa} + \mathrm{IIb} + \mathrm{IIc}) + (\mathrm{IIIa} + \mathrm{IIIb} + \mathrm{IIIc})}$$

$$\mathrm{CBT} = -\log\left(\frac{\mathrm{Ib} + \mathrm{IIb}}{\mathrm{Ia} + \mathrm{IIa}}\right)$$

with Roman numerals corresponding to the GDGT structures shown in Appendix A.

3. Results

3.1. Water column temperature in Huguangyan Maar Lake

Thermistor data for November 2011 to October 2012 show that the vertical temperatures in HML ranged between 15.6–32.1 °C (January–July) for surface water, 15.7–31.5 °C (January–July) for middle depth water, and 15.6–28.1 °C (January–October) for deep water (Fig. 2). In winter (December 2011 to March 2012), the lake is well mixed due to the strong winter monsoon (Wang et al., 2012), causing the whole water column cool to as low as ca. 15.6 °C in January 2012 (Fig. 2). In spring (from March to June) and summer (from June to September), stable thermal stratification developed in the lake and then in autumn (from September to December), the lake went back to mixed conditions (Fig. 2). Therefore, Fig. 2 clearly shows the development of thermal stratification in HML, which began in March and ended in late October 2012. Stable thermal stratification lasted from April to September.

The pH values of the water column were identical, ranging between 7.32–8.34 for surface water, 7.51–8.34 for middle depth water, and 7.35–8.27 for deep water (Fig. 2). The pH value started to decrease in winter, rose again at the end of the winter, remained relatively constant during spring and early summer, then increased in late summer and kept relatively high in autumn (Fig. 2).

3.2. Particulate matter settling fluxes calculated from sediment traps

Fig. 3a shows the vertical and temporal variations of particulate matter fluxes for the duration of the study. From November 2011 to October 2012, the total mass fluxes ranged between 4.0 and 23.9 g $m^{-2}\cdot day^{-1}$, with the maximum in November 2011 and the minimum in October 2012 (Fig. 3a). Fig. 3a shows that the mass fluxes in the deepest trap at 16 m display a feeble seasonal trend. The highest mass flux occurred in late autumn to winter. It decreased during winter, remained constantly low until the end of spring and showed a second peak at the transition to summer (June 2012). Afterwards the mass flux decreased again before it rose to a third peak in September (Fig. 3a). Fig. 3a shows that the mass fluxes of the top sediment trap at 0.5 m and the middle trap at 6.5 m were 0.7–3.8 $g\cdot m^{-2}\cdot day^{-1}$ and 0.6–3.2 $g\cdot m^{-2}\cdot day^{-1}$, respectively. They were both much lower compared to the deep trap. The mass fluxes of these two traps did not exhibit an obvious seasonal trend and were only slightly higher in winter (Fig. 3a). The vertical pattern of particulate matter fluxes indicates that the highest settling mass flux in HML occurred in the deep water (Fig. 3a).

3.3. Distribution and fluxes of GDGTs in sediment trap material

The GDGTs in sediment trap material consisted mostly of branched GDGTs, which accounted for 89.4–97.5% of total GDGTs. For branched GDGTs, the sediment trap material contained a high proportion of GDGT-I, followed by GDGT-II, and GDGT-III present in the lowest amounts (Fig. 4a). Branched GDGTs containing one or two cyclopentyl moieties were less abundant in trap material than those without cyclopentyl moieties (Fig. 4a). The absolute concentration of isoprenoid GDGTs was 16.4–434.8 ng/g. The isoprenoid GDGTs were dominated by GDGT-0 (accounting for 38.3–91.6% of the total isoprenoid GDGTs) and extremely low crenarchaeol. The average GDGT-0/crenarchaeol ratio of settling particles was 14.4 for the 0.5 m traps, 23.8 for the 6.5 m traps and 44.1 for the 16 m traps. The BIT values were high, ranging from 0.99 to 1. The CBT and MBT values were 0.40–0.72 and 0.17–0.62, respectively (Fig. 5).

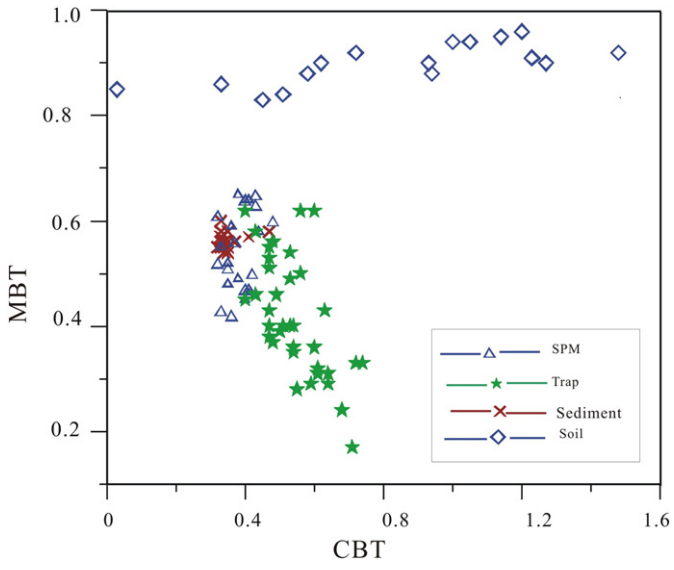

Fig. 5. A cross-plot of CBT (cyclization ratio) and MBT (extent of methylation) in the Huguangyan Maar Lake from traps, suspended particulate matter at the three water depths (0.5 m, 6.5 m and 16 m) during the monitoring period from November 2011 to October 2012, as well as from lake bottom surface sediments (n = 17) and catchment soils (n = 16). The plot reveals that branched GDGTs in lake materials are different to those in surrounding soils.

The estimated pH values were 7.3–8.1 using the equation of Weijers et al. (2007b). Using the equation of Weijers et al. (2007b), the MBT–CBT-derived temperatures for sediment trap materials collected at 0.5, 6.5, and 16 m water depth were 12.5–27.8 °C, 13.5–27.7 °C, and 8.0–22.9 °C, respectively. In contrast, the reconstructed temperatures for the same trap samples using an equation of Sun et al. (2011) were 19.1–30.1 °C, 19.6–30.4 °C, and 15.7–26.6 °C, respectively (Fig. 6a).

The total branched GDGT fluxes determined from sediment traps at all three depths ranged from 3.2 to 24.2 $\mu g \cdot m^{-2} \cdot day^{-1}$, with the highest flux in January and the lowest flux in August 2012. Generally, the total branched GDGT fluxes were higher in winter than in other seasons (Fig. 3b). In the 16 m sediment trap, branched GDGT fluxes ranged from 2.4 to 15.3 $\mu g\ m^{-2}\ day^{-1}$, with the highest flux in March and the lowest flux in August; however, a second less pronounced peak occurred in January, revealing higher flux in winter (Fig. 3b). In the 6.5 and 0.5 m traps, the branched GDGT fluxes ranged from 0.2 to 7.2 $\mu g\ m^{-2}\ day^{-1}$ and from 0.6 to 4.3 $\mu g\ m^{-2}\ day^{-1}$, respectively. At both depths the fluxes of branched GDGTs began to increase in November and reached the maximum value in January. In spring, the fluxes remained constantly low until the end of spring but for the 6.5 m trap, they showed a second peak at the transition to summer (June 2012). Afterwards, the fluxes decreased again and remained constantly low until the end of autumn (Fig. 3b). The fluxes in the 16 m trap were generally higher than those observed in the 6.5 and 0.5 m traps (Fig. 3b). The temporal trends of the total branched GDGT fluxes differed largely from those of the mass accumulation flux within the same trap (Fig. 3a). The peaks in branched GDGT flux in January and March 2012 were delayed by nearly two sampling intervals (corresponding to 60 or 61 days in the trap deployment) relative to the peak in the mass accumulation flux. In contrast, the peaks in the branched GDGT fluxes in July 2012 were delayed only by one sampling interval (corresponding to 30 or 31 days in the trap deployment) relative to the peak in the mass accumulation flux. In September 2012, the peaks were synchronous (Fig. 3).

3.4. Distribution of GDGTs in suspended particulate matter from water samples

The concentrations of branched and isoprenoid GDGTs in suspended particulate matter (SPM) ranged from 1.1 to 6.7 ng L^{-1} and 0.1 to 57.9 ng L^{-1}, respectively (Fig. 7). The fractional abundance of isoprenoid GDGTs was 38.3%–94.6%. The isoprenoid GDGT distribution in SPM was dominated by GDGT-0, which accounted for 78.3%–99.8% of total isoprenoid GDGTs. Crenarchaeol was extremely low. The GDGT-0/crenarchaeol ratios in SPM ranged between 78.9 and 3388.6. In general, the isoprenoid GDGTs were less prevalent in late summer to autumn. In other seasons, they did not show any particular regular pattern (Fig. 7a). Overall, isoprenoid GDGTs in the SPM did not exhibit any clear vertical distribution pattern in the water column during the whole sampling period (Fig. 7a).

In contrast, the concentration of branched GDGTs exhibited better defined vertical distribution pattern in the water column. As a whole, concentrations of branched GDGTs in SPM collected at 16 m were higher than those collected at 6.5 and 0.5 m. The lowest branched GDGT abundance occurred in the SPM collected at 0.5 m water depth (Fig. 7c). Branched GDGTs containing one or two cyclopentyl moieties were less abundant than those without cyclopentyl moieties in SPM. The SPM contains a high proportion of GDGT-I, similar to the

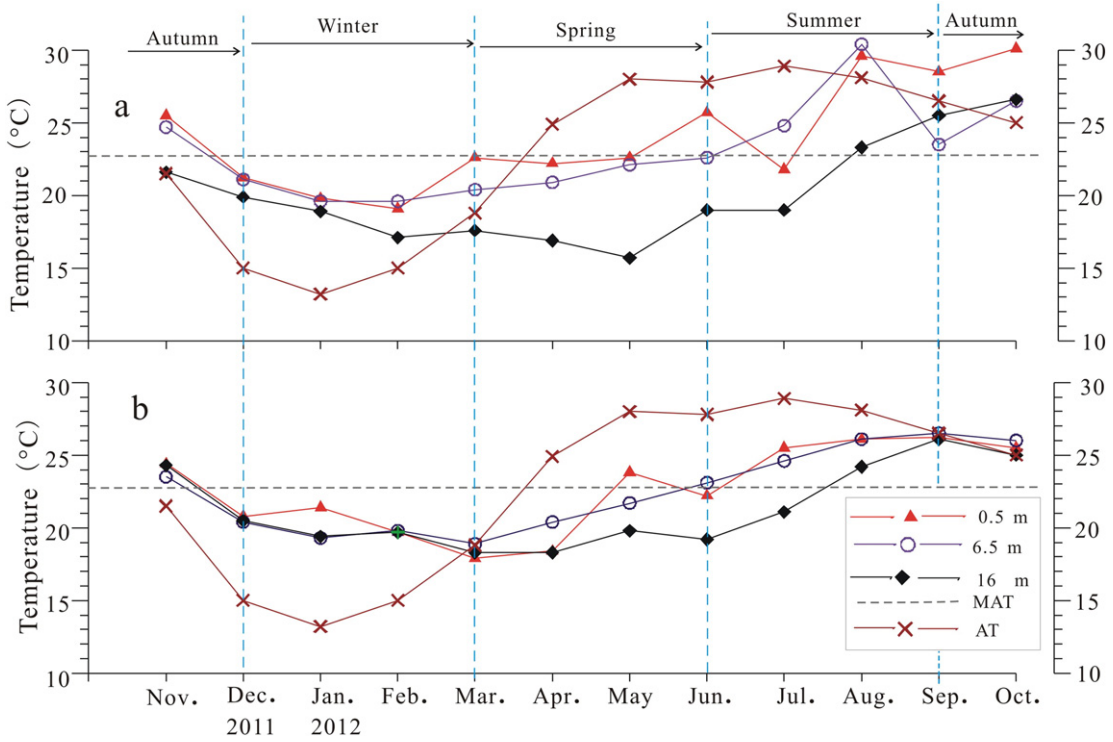

Fig. 6. Vertical and temporal variations of local air temperature (AT) and MBT–CBT-derived temperatures in Huguangyan Maar Lake from a) traps and b) suspended particulate matter at the three water depths (0.5 m, 6.5 m and 16 m) during the monitoring period from November 2011 to October 2012. The variations indicate that local air temperature was higher than the reconstructed temperature during the period March–September 2012, when the stratification occurs in the water column from late spring to mid-autumn in HML, hampering the exchange between the epilimnion and deep water. This trend is reversed for the period November 2011 to March 2012, when strong winter monsoon breaks down stable water column, causing turbulence and the resuspension of material from the slope sediments. MAT: Mean Air Temperature; average of measurements.

distribution of branched GDGTs in sediment trap material (Fig. 4a,b). The relative abundances of GDGT-I, II, and III in SPM were similar among the three sampling depths (Fig. 4b). The BIT values were 0.99–1 (mean 1) and the CBT and MBT values were 0.27–0.50 and 0.42–0.65 for SPM, respectively (Fig. 5). The estimated pH values were 7.6–8.0 and the MBT–CBT-derived temperatures were 11.5–22.2 °C, 12.6–22.1 °C, and 11.8–22.0 °C for water SPM collected at 0.5, 6.5 and 16 m water depth respectively, using the equation of Weijers et al. (2007b). While using the equation of Sun et al. (2011), the reconstructed temperatures for the same SPM were 17.9–26.2 °C, 18.9–26.5 °C, and 18.3–26.1 °C, respectively (Fig. 6b). In general, the concentrations of total branched GDGTs in SPM were slightly higher in winter than in other seasons. However, the highest concentration occurred in June 2012 for the SPM from 16 m depth (Fig. 7c). In August to October, when there are very low abundances of isoprenoid GDGTs, the branched GDGTs also are the lowest (Fig. 7a,c).

3.5. GDGTs in lake bottom surface sediments

The concentrations of isoprenoid and branched GDGTs in the 17 lake bottom sediment samples range from 66.3 to 165.2 ng g^{-1} and from 725.1 to 2008.6 ng g^{-1} dry weight (dw), respectively. The GDGT distributions in the sediments were dominated by branched GDGTs (88.2–93.4%, mean 91.6%). The isoprenoid GDGTs were dominated by GDGT-0, which accounted for 49.6–70.4% of the total isoprenoid GDGTs. Followed by crenarchaeol, which accounted for 10.8–21.0% of the total isoprenoid GDGTs. The GDGT-0/crenarchaeol ratios were 2.4–6.2. Using the calibration of Castañeda and Schouten (2011), the TEX_{86} reconstructed temperature for the surface sediment was in the range of 6.2–12.9 °C.

For branched GDGTs, the lake bottom surface sediments contained a high proportion of GDGT-I, followed by GDGT-II (Fig. 4c). Branched GDGTs containing one or two cyclopentyl moieties were less abundant in lake bottom sediments than those without cyclopentyl moieties, and they exhibited a relative composition identical to those of the trap material and the SPM of water (Fig. 4a, b and c).

The BIT values varied from 0.97 to 0.99 (mean 0.98), and the CBT and MBT values were 0.32–0.47 and 0.54–0.60, respectively (Fig. 5). The reconstructed pH values and MBT–CBT-derived temperatures following the equation of Weijers et al. (2007b) were 7.6–7.9 and 17.5–20.7 °C. In contrast, the reconstructed temperatures for the lake bottom surface sediments using an equation of Sun et al. (2011) were 22.5 to 25.0 °C, with a mean value 23.4 °C.

3.6. GDGTs in catchment soils

The concentrations of isoprenoid and branched GDGTs ranged from 1.8 to 38.8 ng g^{-1} and from 33.2 to 259.2 ng g^{-1} dw, respectively, in the 16 soil samples. Clearly, the GDGT compositions are dominated by branched GDGTs (up to 99.2% of total GDGTs) (Table 1). Isoprenoid GDGTs in soils were dominated by crenarchaeol, which constituted 36.5–59.0% of the total isoprenoid GDGTs. Next is GDGT-0, which

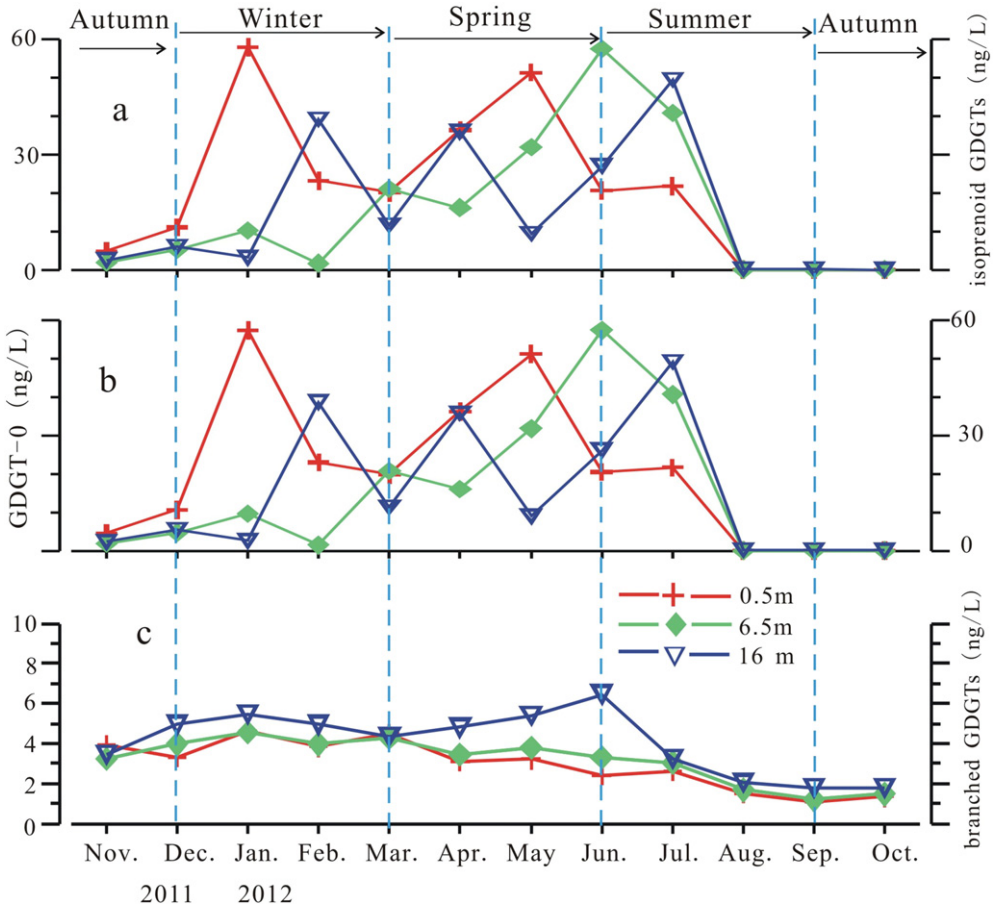

Fig. 7. Annual variations in concentration in Huguangyan Maar Lake of: a) isoprenoid GDGTs, b) GDGT-0, and c) branched GDGTs in suspended particulate matter at three different water depths during the monitoring period from November 2011 to October 2012. Isoprenoid GDGTs dominated by GDGT-0 in the SPM did not exhibit any vertical pattern in the water column, while branched GDGTs exhibited an obvious vertical and seasonal distribution pattern in the water column, with higher concentrations in deeper water and winter season.

Table 1
Absolute concentrations of individual branched GDGTs, total branched GDGTs and total isoprenoid GDGTs, BIT, CBT and MBT, and pH, as well as MBT–CBT-reconstructed mean annual air temperature (MAAT) in catchment soils of Huguangyan Maar Lake.

Sample no.	Individual branched GDGT concentration (ng/g)									Branched GDGT concentration (ng/g)	Isoprenoid GDGT concentration (ng/g)	BIT	CBT	MBT	MBT′	pH[a])	pH[b])	MAAT (°C)[a]	MAAT(°C)[b]
	III	IIIb	IIIc	II	IIb	IIc	I	Ib	Ic										
S1	1.4	0.1	–	12.7	2.4	0.7	113.8	12.3	3.4	146.8	6.7	0.99	0.94	0.88	0.88	6.3	6.1	29.3	22.9
S2	0.2	–	–	4.8	0.7	0.08	81.9	8.0	1.8	97.5	4.8	0.97	1.00	0.94	0.94	6.1	5.9	31.6	24.3
S3	0.4	0.04	–	8.3	1.4	0.2	196.6	13.4	3.4	223.7	1.8	1.00	1.14	0.95	0.95	5.8	5.7	30.9	23.9
S4	0.4	–	–	3.8	1.1	0.1	30.0	7.7	1.4	44.4	7.5	0.89	0.58	0.88	0.88	7.2	6.8	32.4	24.8
S5	1.1	0.1	–	16.7	3.9	0.2	152.2	36.6	8.6	219.4	33.7	0.90	0.62	0.90	0.90	7.1	6.7	33.1	25.2
S6-1	0.2	–	–	2.6	0.3	0.1	26.4	3.0	0.6	33.2	4.1	0.93	0.93	0.90	0.90	6.3	6.1	30.4	23.6
S6-2	0.3	–	–	5.0	0.5	0.03	76.7	6.9	1.9	91.3	8.5	0.94	1.05	0.94	0.94	6.0	5.8	31.0	23.9
S6-3	0.1	–	–	3.0	0.3	–	71.0	4.4	1.4	80.2	9.2	0.93	1.20	0.96	0.96	5.6	5.5	30.6	23.7
S6-4	0.3	–	–	5.2	1.0	0.1	60.3	11.5	2.8	81.4	21.8	0.84	0.72	0.92	0.92	6.9	6.5	33.1	25.2
S7	1.8	0.1	–	17.2	4.8	0.6	91.5	29.1	6.0	151.2	16.7	0.94	0.51	0.84	0.84	7.4	6.9	31.0	23.9
S8	3.4	0.2	–	26.7	7.7	0.9	135.1	50.1	9.4	233.6	22.1	0.94	0.45	0.83	0.83	7.6	7.0	31.4	24.1
S9	0.9	–	–	19.7	1.0	0.3	228.4	7.3	1.7	259.2	13.7	0.98	1.48	0.92	0.92	4.9	5.0	25.9	20.8
S10	0.7	–	–	12.4	1.0	0.2	120.2	6.2	1.3	141.9	17.3	0.95	1.27	0.90	0.90	5.4	5.4	27.0	21.5
S11	1.5	1.0	–	14.4	5.6	0.4	83.5	39.7	13.6	158.8	38.8	0.81	0.33	0.86	0.86	7.9	7.2	33.8	25.6
S12	0.6	0.1	–	6.5	2.5	0.2	32.7	16.9	4.4	64.0	11.7	0.87	0.30	0.85	0.85	8.0	7.3	33.3	25.3
S13	0.1	–	–	3.6	0.4	0.1	38.7	2.1	0.4	45.4	6.1	0.95	1.23	0.91	0.91	5.5	5.5	27.8	22.0
Mean	0.8	0.1	–	10.2	2.2	0.3	96.2	16.0	3.9	129.5	6.7	0.93	0.86	0.90	0.90	6.5	6.2	30.8	23.8

– under the limit of detection.
[a] Calculated according to Weijers et al. (2007b).
[b] Calculated according to Peterse et al. (2012).
MAAT Mean Annual Air Temperature; calculated from GDGTs.

accounts for 3.3–20.5% of the total isoprenoid GDGTs. The GDGT-0/crenarchaeol ratios were 0.1–0.5.

Among branched GDGTs, the average relative abundances of GDGTs-I, II, and III in soils were 89.5%, 9.8%, and 0.7%, respectively (Fig. 4d). For GDGT-III compounds, GDGT-IIIb and GDGT-IIIc were not detected. The BIT values ranged from 0.81 to 1.0 (mean 0.93), and the CBT and MBT values were 0.30–1.48 and 0.85–0.96, respectively. The reconstructed MAT based on soil MBT–CBT calibration (Weijers et al., 2007b) ranged from 25.9 to 33.8 °C, and the pH values were 4.9–8.0 (Table 1). The MAT estimates calculated according to the revised calibration by Peterse et al. (2012) were 21.5–25.6 °C, and the pH values varied between 5.0 and 7.3 (Table 1).

4. Discussion

4.1. Seasonal changes in flux and concentration of branched GDGTs and water stratification state

The flux of branched GDGTs from the monthly sediment trap samples showed distinct seasonal variations. Fluxes of total mass of particulate matter were higher in late autumn to early winter, with the highest in November 2011 (Fig. 3a). The values for branched GDGTs were significantly higher in winter than in other seasons (Fig. 3) with the highest values in January 2012 (Fig. 3b). During late autumn to winter in the HML region, the East Asian winter monsoon regime is dominant, with high wind speeds inducing turbulent mixing, which results in an isothermal water column (Fig. 2) (Wang et al., 2008, 2012). Hence, during periods of strong wind, turbulence in the water column breaks down the thermal stratification in the lake, causing nutrient-rich bottom water to mix with surface water (Pilskaln and Johnson, 1991; Zhang et al., 2008). These conditions favor algal productivity (especially diatoms) in HML (Zhang et al., 2008), which might result in an increase in the total mass flux (Fig. 3a).

On the other hand, the seasonal difference in dust flux may affect the overall mass flux. Yancheva et al. (2007) concluded that the strong northerly winter monsoon winds delivered more wind-blown material (dust) into HML and caused turbulence in the water column. Thus, the high mass flux in November–December 2011 and January 2012 might be due to a higher dust input during these months (Yancheva et al., 2007) as stronger East Asian winter monsoon occurred in winter 2011/2012 (Sun et al., 2012). However, it has been found that GDGTs are not transported through the atmosphere (Hopmans et al., 2004), hence, higher levels of atmospheric dust does not directly imply high GDGTs flux. The peaks of particle mass flux and branched GDGTs flux are asynchronous in HML (Fig. 3), which further support that more atmospheric dust does not directly cause high GDGTs flux.

Fig. 2 clearly shows the development of thermal stratification in HML in 2011–2012. Thermal stratification began in March and ended in late October 2012. The onset of thermal stratification corresponded to the decline in the mass flux of particulate matter and the decrease of branched GDGTs in surface and middle depth water. In late May 2012, a strong thunderstorm gale occurred in the Zhanjiang area and lasted for several days. This strong wind caused the mixing of the water column, which resulted in increased particulate matter mass flux in June (Fig. 3a). However, the increase of particulate matter mass flux was only seen in the 16 m depth traps. This might be due to the intensity of the thunderstorm gale, which promoted the exchange between the epilimnion and deep water and relatively more resuspended material from lake bottom surface sediment that was captured. The corresponding peak flux of branched GDGTs occurred in July and was only seen in the 6.5 m traps (Fig. 3b). While resuspension of lake bottom sediments may have occurred, it is not clear why the flux of branched GDGTs increased only in the middle depth traps. On the whole, the time lag between the maximal fluxes of branched GDGTs and mass particulate matter suggests that the bacteria that produce branched GDGTs thrive after algal blooms in HML. Thus, the concentrations of branched GDGTs in the water column are likely influenced by seasonal variability in primary production in the upper layers.

The concentrations of branched GDGTs in the SPM also exhibited certain seasonality in HML. They were slightly higher in winter than in other seasons. However, the highest concentration occurred in June 2012 (Fig. 7c), especially for the 16 m traps, which is similar to that of settling particles. The lowest concentration of branched GDGTs in SPM occurred in August to October, when there are barely detectable concentrations of isoprenoid GDGTs, which is different from that of settling particles. As the SPM was collected at the given short time and the settling particles were collected over relatively longer periods, the temporal and vertical patterns of branched GDGTs might differ. Indeed, in the case described here they do.

4.2. Sources of GDGTs in Huguangyan Maar

4.2.1. Branched GDGTs

This study reveals that branched GDGTs constituted the main component of total GDGTs in settling particles, sediments, and catchment soil. This is different from observations from Lake Challa in equatorial Africa and Lake Lucerne in Switzerland, where branched GDGTs represented only a small fraction of all GDGTs (Sinninghe Damsté et al., 2009; Blaga et al., 2011). However, at HML isoprenoid GDGTs dominated in most of the water SPM, and branched GDGTs only dominated in three months (August–October 2012). The molecular distribution of branched GDGTs in settling particles, SPM, and surface sediments of HML was very similar, but this distribution pattern differed from that in the catchment soil samples (Fig. 4). The fractional abundances of GDGT-IIa and GDGT-IIIa were higher in water column and lake bottom sediment samples than in the soils (Fig. 4). Consequently, GDGT-IIa and GDGT-IIIa in the lake must have an additional source, likely *in situ* production. In comparison with the fractional abundances of GDGT-IIIa in settling particles and sediment, the GDGT-IIIa abundance in lake sediments was slightly lower than in settling particles, suggesting that GDGT-IIIa might originate from *in situ* production in the water column. A close examination of Fig. 4a and b reveals that the GDGT-IIa and GDGT-IIIa abundances show a slight decreasing trend from the deeper sampling depth at 16 m to the shallower ones at 6.5 m and 0.5 m, indicating that these two isomers were mainly produced in the deeper part of the water column. These findings suggest that a significant proportion of the branched GDGTs in the HML lacustrine setting might originate from *in situ* production in the lake rather than from soil.

Furthermore, the CBT-derived pH values of settling particles, sediments, and SPM were 7.3–8.1, 7.6–7.9 and 7.6–8.0, resembling those measured for the lake water (7.32–8.34, Fig. 2). Therefore we conclude that the branched GDGTs in HML are mainly derived from *in situ* production and have been influenced by water column conditions in HML.

Further information about the provenance of the branched GDGTs in the lake was obtained by comparing their distributions, which can be expressed in terms of MBT and CBT. The cross-plot of these two ratios (Fig. 5) shows the substantial difference in the branched GDGT composition between lake materials and soils. The distribution of branched GDGTs in soils collected close to the lake was relatively uniform with regard to the MBT values of ca. 0.90. But they show a wide range of CBT ratios (from 0.03 to 1.48). In comparison, the branched GDGTs from lake materials exhibited a wide range of MBT values (from 0.17 to 0.65) and a relatively small range of CBT ratios of ca. 0.45 (Fig. 5). The settling particles sampled through the year at different water depths also showed a wide range of MBT values. In contrast, the distribution of branched GDGTs in surface sediments was relatively uniform, with MBT values of ca. 0.56 and CBT ratios of ca. 0.35. Moreover, the BIT values were 0.97 to 1.0 for settling particles, SPM, and surface sediments, which were higher than those for part of the soils (with BIT values in the range of 0.81 to 0.84). These results also indicate that the branched GDGTs in HML do not originate only from catchment soils, but rather from *in situ* production of branched GDGTs in the water column or in the sediment.

In order to obtain statistical data on the difference between GDGTs of the samples from HML, cluster analysis was performed on the branched GDGT lipid composition of settling particles, SPM, surface sediments, and soils. The branched GDGTs of settling particles, SPM, and surface sediments clustered into one group, whereas the branched GDGTs of soils formed a second group (Fig. 8). This distinction further supports the idea that branched GDGTs in HML are primarily autochthonous. Moreover, the vertical variation of branched GDGTs in SPM and settling particles at different water depths revealed that the highest abundance/flux of branched GDGTs occurred at the deepest water sampling site (Figs. 3b and 7c). The most likely explanation for this observation is that more branched GDGTs originated from the deep water and/or the water sediment interface. Also Blaga et al. (2011) observed that the concentrations of branched GDGT were higher at greater depths than in shallow depths in Lake Lucerne, and suggested that deep water *in situ* production of branched GDGTs was the main cause. Relatively higher abundance/flux of branched GDGTs in the deeper water samples suggests that the source microorganisms for branched GDGTs are more abundant in the deep water in HML.

Autochthonous and allochthonous branched GDGTs are the two sources of branched GDGTs in the HML sedimentary GDGT pool. Thus, the BIT ratios in sediment provide a record of these two sources. Referring to the mixing model of $\delta^{13}C_{org}$ in marine sediments (Shultz and Calder, 1976), the two end-member model based on the BIT ratio in lake sediments (BIT_{sed}) would be:

$$BIT_{sed} = BIT_{lake} \times GDGT_{lake} + BIT_{soil} \times GDGT_{soil}. \quad (1)$$

For HML, the mean BIT ratio (1.0) for the SPM from three depths collected during the one-year period was used as the end-member BIT_{lake} value. The mean BIT ratio of catchment soils (0.93) was used as the soil end-member BIT_{soil} value. Adopting the above end-member values, the relative percentage of lake-derived branched GDGTs (f %) in lake bottom surface sediments of HML was estimated using the following equation:

$$GDGT_{lake}\ [\%] = \frac{BIT_{sed} - BIT_{soil}}{BIT_{lake} - BIT_{soil}} \times 100, \text{and } GDGT_{soil} = 1 - GDGT_{lake}. \quad (2)$$

The resulting estimates for the contribution of the lake-derived branched GDGTs were 58%–81%, with a mean value 70%. Although this estimate may not be so accurate due to the relatively low precision of determination the end-member BIT. These data suggest that the majority of the branched GDGTs in HML sediments are lake-derived.

4.2.2. Isoprenoid GDGTs

The fractional abundances of isoprenoid GDGTs in settling particles and surface sediments were similar. They were lower than those of the branched GDGTs. However, the fractional abundances of isoprenoid GDGTs in most of the water SPM were higher than those of the branched GDGTs. The distribution of isoprenoid GDGTs in settling particles at the different water depths was identical, indicating the same source(s) for these components. This distribution, dominated by GDGT-0 and extremely low crenarchaeol, strongly suggests that isoprenoid GDGTs were mainly derived from methanogens, which produce predominantly GDGT-0 (Blaga et al., 2009), and were not from Thaumarchaeota in HML. Thaumarchaeota are the only archaea identified as producers of crenarchaeol (Sinninghe Damsté et al., 2002; Pitcher et al., 2010; Spang et al., 2010). The average GDGT-0/crenarchaeol ratio of settling particles showed the following depth profile: surface < middle < bottom, indicating that more GDGT-0 was produced in deeper part of the water column. Indeed, the deeper water is more anoxic (Guo et al., 2002) and favors the growth of methanogens. Moreover, the GDGT-0/crenarchaeol ratios for the surficial lake bottom sediment samples (2.4–6.2) were substantially lower than that of the settling particles. This was caused by the higher content of crenarchaeol in bottom sediments than in the water. Thaumarchaeota are nitrifiers (Könneke et al., 2005; Leininger et al., 2006) and tend to live close to areas where ammonium is released, which is consistent with the inferred physiology of Thaumarchaeota (Könneke et al., 2005; Leininger et al., 2006). It was found that ammonium released from the bottom sediment is an important replenishment of N in HML (Zhang et al., 2008).

The fractional abundances of isoprenoid GDGTs in most water SPM samples were quite different from those in settling particles. For example the abundances of isoprenoid GDGTs in SPM were higher than those in settling particles. This difference was observed previously. Huguet et al. (2008), Schouten et al. (2013 and references therein), ascribe the

difference to the more rapid degradation of isoprenoid GDGTs than branched GDGTs adsorbed onto fine particles during their slow settling through the water column. Sinninghe Damsté et al. (2009) offer an alternative explanation, of higher abundance of branched GDGTs produced at the surface and are adsorbed to larger fast sinking particles more easily captured in the sediment trap.

At HML branched GDGTs occur in higher abundance in settling particles in the deepest samples. However, Fig. 7 shows that the higher fractional abundance of isoprenoid GDGTs in SPM is related to the higher content of GDGT-0. The temporal and vertical variation trend of isoprenoid GDGTs is the same as that of GDGT-0 (Fig. 7a,b). Therefore, these features suggest that *in situ* production of GDGT-0 in the water column of HML took place. According to the review by Schouten et al. (2013), the capability to biosynthesize GDGT-0 is common in the archaeal domain. It remains unclear which type of archaea is the likely source of GDGT-0 in the water column in HML.

Crenarchaeol was found to be the main isoprenoid GDGTs in the catchment soils, similar to previous findings in European lakes (Blaga et al., 2009; Naeher et al., 2014). The presence of crenarchaeol and other isoprenoid GDGTs in both the soils and the lake suggests that the isoprenoid GDGTs in HML are not only derived from Thaumarchaeota in the water column (Naeher et al., 2014), but also from soil Thaumarchaeota living in the soils surrounding the lake. However, the BIT values of some soils were typically <0.9 (Table 1), whereas the BIT index is >0.9 in the SPM, settling particles and sediment. This further supports the notion that the lake sediments receive both soil-derived crenarchaeol and aquatically produced branched GDGTs (Naeher et al., 2014), and confirms the idea that the BIT index is not adequate for determining the input of soil organic matter in HML.

Blaga et al. (2009) suggested that if the GDGT-0/crenarchaeol ratio is >2, a non-Group I crenarchaeotal origin is evident for GDGT-0, and in such a case, it is not appropriate to calculate TEX_{86} values and infer past lake water temperatures. As all the GDGT-0/crenarchaeol ratios in HML are >2, TEX_{86} values cannot be used in the reconstruction of water temperature in HML.

4.3. GDGTs inferred temperatures in HML

As discussed above, TEX_{86} values cannot be used in the reconstruction of temperature in HML. Indeed, the TEX_{86} reconstructed temperatures for the lake bottom surface sediment samples were 6.2–12.9 °C. These values are much lower than the measured local air temperature (13.2–29.0 °C) and lake water temperature (12.6–29.1 °C, Wang et al., 2012). Moreover, the average value of MAT for the last 45 years, for the town of Zhanjiang (15 km from Huguangyan) is 23.1 °C (Mingram et al., 2004). Therefore, we do not discuss the temperatures based on TEX_{86} values here.

For soil surrounding HML, MAT and pH values calculated using the original global soil calibration developed by Weijers et al. (2007b) and the revised calibration by Peterse et al. (2012) were quite different (Table 1). As the local average MAT value for the past 45 years is 23.1 °C, it seems that the branched GDGT-derived temperature estimates by the revised calibration proposed by Peterse et al. (2012) for soil, were in a range similar to that of local air temperature. The calculated pH values (5.0–7.3), were in the range of soil pH measured in the Zhanjiang area (Guo et al., 2011). The different temperature estimates based on these two calibration models might be due to the absence of GDGT-IIIb and GDGT-IIIc compounds in our samples. The model of Peterse et al. (2012) used MBT′ instead of MBT in the model of Weijers et al. (2007b), which was based on the absence of GDGT-IIIb and GDGT-IIIc compounds. Therefore, in the absence of the GDGT-IIIb and GDGT-IIIc compounds, it is more practical to use the calibration proposed by Peterse et al. (2012) for soil MAT estimate.

The branched GDGTs have been regarded as of potential use as temperature proxy indicators in various lacustrine settings (Tierney et al., 2010b; Zink et al., 2010). Application of the temperature proxy to lake sediments, however, showed that the distribution of branched GDGTs in the sediments of Lake Challa in equatorial West Africa (Sinninghe Damsté et al., 2009), and Lake Towuti in Indonesia (Tierney and Russell, 2009) differs from that in the surrounding soils. Therefore, *in situ* production was suggested as a source of branched GDGTs in the lake, in addition to those derived from soils surrounding the lake. This *in situ* production complicates the application of the MBT–CBT proxy in lacustrine settings, and tends to result in a large underestimation of MAT (Tierney et al., 2010b; Zink et al., 2010; Sun et al., 2011; Pearson et al., 2011). Therefore, Schouten et al. (2013) suggested that local or regional calibrations may be necessary for reconstructing absolute air temperatures. Indeed, several lake-specific calibrations have been developed which incorporated the potential aquatic input of branched GDGTs and thus enable the reconstruction of paleotemperatures based on branched GDGTs in lake sediments (e.g. Tierney et al., 2010b; Sun et al., 2011; Pearson et al., 2011; Loomis et al., 2012). This resulted in a better agreement between temperatures calculated for lacustrine branched GDGTs, and measured temperatures.

As shown above, the *in situ* production of branched GDGTs in the HML lake water column and/or sediments contributed a substantial portion of the total branched GDGTs in the sediment. Therefore, the application of the MBT–CBT-paleothermometer in HML requires a calibration based on the distribution of branched GDGTs in the lake bottom surface sediment samples rather than in the soil samples. Indeed, in this research, the MBT–CBT-derived temperatures based on the calibration of Weijers et al. (2007b) were lower than those based on the calibration of Sun et al. (2011) for sediment trap materials, SPM and lake bottom

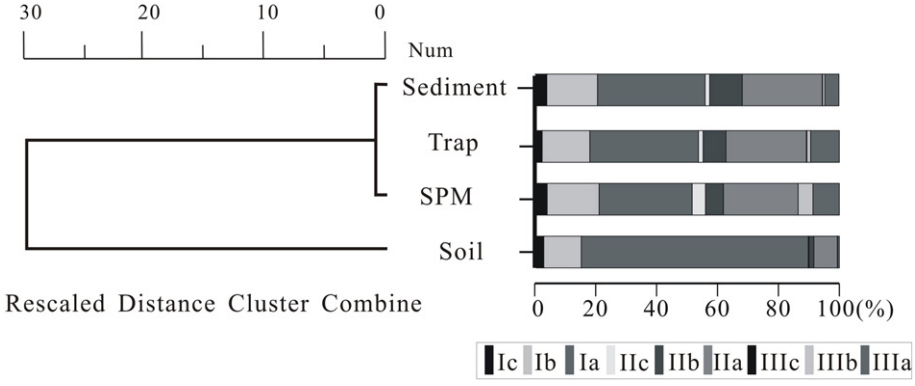

Fig. 8. Cluster analysis of nine branched GDGTs (for structure see Appendix A) in the Huguangyan Maar Lake from traps and suspended particulate matter at three different water depths during the monitoring period from November 2011 to October 2012, as well as from lake bottom surface sediments (n = 17) and catchment soils (n = 16). The figure shows that surface sediments, traps, and SPM are in the same group, whereas soils are in the other group, indicating that branched GDGTs in HML do not originate only from catchment soils; *in situ* production in the lake represents an additional significant source.

surface sediments. Therefore, the sediment-based MBT–CBT calibration model of Sun et al. (2011) was used to calculate the paleotemperature, as this calibration model given below, was based on lakes from China and Nepal, covering a climate gradient from the tropics to the temperate zone:

$$T\,(^{\circ}C) = 3.949 - 5.593 \times CBT + 38.213 \times MBT \left(n = 100, p<0.0001, R^2 = 0.73, \text{and RMSE} = 4.27\ ^{\circ}C\right)$$

The MBT–CBT-derived temperatures for the sediment trap materials and SPM are shown in Fig. 6. The mean temperature estimates were 22.5 °C and 23.4 °C for traps and SPM respectively. The difference in MBT–CBT-derived temperature between 0.5 m and 16 m is considerable (up to 6.9 °C) for settling particles, especially during the period of March to September 2012 (Fig. 6a). This might be caused by the stratification of the water column. In comparison, the difference in temperature between 0.5 m and 16 m is relatively small (up to 4.4 °C) for SPM (Fig. 6b), possibly because the SPM was collected at the given short time (from 8 am to 4 pm) and the settling particles were collected over longer periods of one month, the SPM samples contain more material which could be affected by instantaneous mixing, while the samples of settling particles represent water column processes over sampling of one month. In that case, the SPM collected at different depths would show some homogeneity. However, the reconstructed temperature showed similar temporal and vertical patterns for settling particles and SPM, suggesting that the same factors controlled the branched GDGTs produced in the water column.

For the period March–September 2012, the measured air temperature was higher than the reconstructed temperature for SPM and most of the settling particles. However, the settling particles for 0.5 m and 6.5 m depths showed higher reconstructed temperatures for March and August, and only 0.5 m showed higher reconstructed temperature for September. Stratification in HML occurs in the water column from late spring to mid-autumn (Fig. 2), hampering the exchange between the epilimnion and the deeper waters. Such long term stratification may cause anoxia and reduction in primary productivity due to the decrease in nutrient replenishment from bottom surface sediment to surface water. In this case, the branched GDGT-producing microorganisms decreased and would tend to live in the relatively cooler deep water. As shown in Fig. 3b, the concentration of branched GDGTs are anyway higher in the deeper water. Thus, the reconstructed temperature is lower than air temperature.

In October the measured air temperature was lower than all the calculated temperatures for the three different depths. This trend is also observed in the period November 2011 to early March 2012 (Fig. 6). During the late autumn to winter season in the HML region, the East Asian winter monsoon regime is dominant, with high wind speeds inducing turbulent mixing in the whole water column. In that way, a portion of the settling particles and SPM might be derived from slope sediments which might record the temperatures that prevailed earlier. At the same time, i.e. during periods of strong winds, turbulence in the water column breaks down the thermal stratification in the lake, causing nutrient-rich bottom water to mix with surface water (Pilskaln and Johnson, 1991; Zhang et al., 2008). These conditions favor the growth of algae (especially diatoms) in the upper layers (Zhang et al., 2008) and also the productivity of bacteria that produce branched GDGT in HML (Fig. 3b). In this case, the branched GDGT-produced bacteria would tend to thrive in the relatively shallow water. Therefore, the MBT–CBT-derived temperatures will record the temperatures in upper water layers, which would be relatively higher. These two aspects might be the reasons for obtaining reconstructed temperature values being higher than the measured ones during this period.

However, the annual mean of the branched GDGT-derived temperature estimates (22.5 °C for sediment traps and 23.4 for SPM) were similar to the measured local mean annual air temperature (22.7 °C). Moreover, the reconstructed temperatures for lake bottom surface sediments ranged from 22.5 to 25.0 °C, with a mean value 23.4 °C using the equation of Sun et al. (2011). These temperature estimates bracket the local MAAT value of 23.1 °C for the past 45 years. The branched GDGT signal of the lake bottom surface sediments is the sum of all GDGT signals in the overlying waterbody. Therefore, although the main production of branched GDGTs takes place in deeper parts of the HML (Fig. 3b), no mixing effects on the GDGT temperature were detected in the signal in 0.5 m depth (Fig. 6).

These results suggest that MBT–CBT proxy can reflect local air temperature in HML on annual or longer time scales and it is valid to use the temperature reconstruction based on branched GDGTs in HML to derive the record of paleotemperatures.

5. Conclusions

In the present study, the temporal and vertical variations in concentrations and fluxes of GDGTs were investigated in Huguangyan Maar Lake (HML) in SE China over the course of an annual cycle November 2011 to October 2012. GDGTs in lake bottom sediment and in surrounding soil were also analyzed. The results showed that:

1) Sediment trap material and lake bottom sediments were dominated by branched GDGTs with a minor contribution of isoprenoid GDGTs, while most of the water suspended particulate matter (SPM) was dominated by isoprenoid GDGTs.
2) The molecular distribution pattern of branched GDGTs in SPM, settling particles and surface sediments of HML were very similar, but they differed from those of samples of soil surrounding the lake, indicating that the branched GDGTs within the lake are derived primarily from *in situ* production in the lake.
3) *In situ* production of branched GDGTs takes place mainly in the deeper part of the water column and/or at the sediment–water interface and shows seasonal variations. The primary production in the upper water mass is likely to be influenced by seasonal changes of the nutrient in the water column.
4) The maximum concentration and flux of branched GDGTs occurred during winter time when the water column is well mixed and resuspension of slope sediment takes place as a result of the strong East Asian winter monsoon.
5) Although the MBT–CBT-derived temperatures using the calibration of Sun et al. (2011) were different for settling particles and SPM. Also, the measured air temperature (AT) at the sampling date differed from the temperature calculated using this proxy for the samples collected on the same day. However, on an annual or longer time scale the MBT–CBT proxy provides a good estimate of local AT at HML. This is demonstrated by the agreement between the MBT–CBT based temperature estimate of HML bottom sediments of 22.5 to 25.0 °C and the average of the local measured AT of 23.1 °C for the preceding 45 years. Thus, this study shows that although the East Asian monsoon affects the concentration and flux of GDGTs in the water column on a seasonal time scale, it is feasible to use the MBT–CBT proxy for paleothermometry in HML and similar lacustrine settings on annual or longer time scales.

Acknowledgments

We thank H.C. Kuang, P. Chen from GIG, and X. X. Dong from IGG for providing assistance during the sampling. Special thanks to Profs. Kai Mangelsdorf and Philip Meyers, and Editor Michael E. Böttcher for helpful comments on earlier drafts of the manuscript. This work was financially supported by a GIGCAS 135 project Y234091001, National Natural Science Foundation of China (Nos. 41503079 and 41372110) and this is also Contribution No. IS-2161 from GIGCAS.

Appendix A. The chemical structures of GDGTs and internal standard discussed in the text

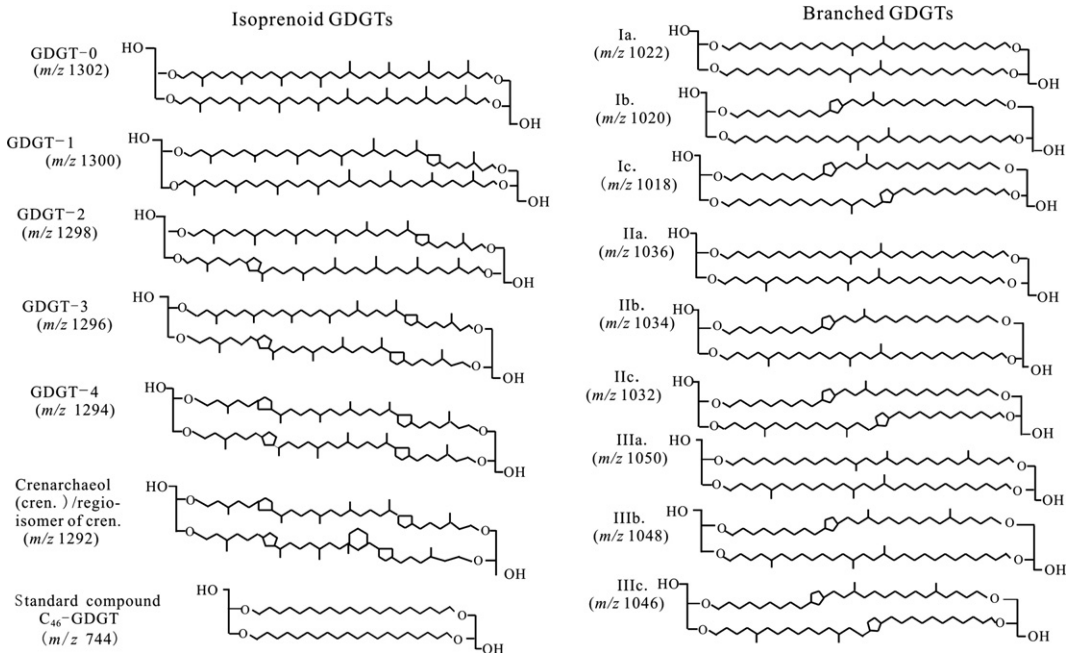

Appendix B. Supplementary data

Supplementary data to this article can be found online at http://dx.doi.org/10.1016/j.chemgeo.2015.11.008.

References

Blaga, C.I., Reichart, G.J., Heiri, O., Sinninghe Damsté, J.S., 2009. Tetraether membrane lipid distributions in water-column particulate matter and sediments: a study of 47 European lakes along a north–south transect. J. Paleolimnol. 41, 523–540.

Blaga, C.I., Reichart, G.J., Vissers, E.W., Lotter, A.F., Anselmetti, F.S., Sinninghe Damsté, J.S., 2011. Seasonal changes in glycerol dialkyl glycerol tetraether concentrations and fluxes in a perialpine lake: implications for the use of the TEX_{86} and BIT proxies. Geochim. Cosmochim. Acta 75, 6416–6428.

Castañeda, I.S., Schouten, S., 2011. A review of molecular organic proxies for examining modern and ancient lacustrine environments. Quat. Sci. Rev. 30, 2851–2891.

Chu, G.Q., Liu, J.Q., Sun, Q., Lü, H.Y., Gu, Z.Y., Wang, W.Y., Liu, T.S., 2002. The 'Mediaeval Warm Period' drought recorded in Lake Huguangyuan, tropical South China. The Holocene 12, 511–516.

Fawcett, P.J., Werne, J.P., Anderson, R.S., Heikoop, J.M., Brown, E.T., Berke, M.A., Smith, S.J., Goff, F., Donohoo-Hurley, L., Cisneros-Dozal, L.M., Schouten, S., Sinninghe Damsté, J.S., Huang, Y.S., Toney, J., Fessenden, J., WoldeGabriel, G., Atudorei, V., Geissman, J.W., Allen, C.D., 2011. Extended megadroughts in the southwestern United States during Pleistocene interglacials. Nature 470, 518–521.

Fuhrmann, A., Mingram, J., Lückea, A., Lu, H., Horsfield, B., Liu, J., Negendank, J.F.W., Schleser, J.H., Wilkes, H., 2003. Variations in organic matter composition in sediments from Lake Huguang Maar (Huguangyan), south China during the last 68 ka: implications for environmental and climatic change. Org. Geochem. 34, 1497–1515.

Guo, Z.F., Liu, J.Q., Chu, G.Q., Negendank, J.F.W., 2002. Composition and origin of tephra of the Huguangyan Maar Lake. Quat. Sci. 22, 266–272 (in Chinese with English abstract).

Guo, Z., Wang, J., Chai, M., Chen, Z., Zhan, Z., Zheng, W., Wei, X., 2011. Spatiotemporal variation of soil pH in Guangdong Province of China in past 30 years. Chin. J. Appl. Ecol. 22 (2), 425–430.

Hopmans, E.C., Weijers, J.W.H., Schefuss, E., Herfort, L., Sinninghe Damsté, J.S., Schouten, S., 2004. A novel proxy for terrestrial organic matter in sediments based on branched and isoprenoid tetraether lipids. Earth Planet. Sci. Lett. 224, 107–116.

Huguet, C., Hopmans, E.C., Febo-Ayala, W., Thompson, D.H., Sinninghe Damsté, J.S., Schouten, S., 2006. An improved method to determine the absolute abundance of glycerol dibiphytanyl glycerol tetraether lipids. Org. Geochem. 37, 1036–1041.

Huguet, C., de Lange, G.J., Gustafsson, Ö., Middelburg, J.J., Sinninghe Damsté, J.S., Schouten, S., 2008. Selective preservation of soil organic matter in oxidized marine sediments (Madeira Abyssal Plain). Geochim. Cosmochim. Acta 72, 6061–6068.

Könneke, M., Bernhard, A.E., de la Torre, J.R., Walker, C.B., Waterbury, J.B., Stahl, D.A., 2005. Isolation of an autotrophic ammonia-oxidizing marine archaeon. Nature 437, 543–546.

Leininger, S., Urich, T., Schloter, M., Schwark, L., Qi, J., Nicol, G.W., Prosser, J.I., Schuster, S.C., Schleper, C., 2006. Archaea predominate among ammonia-oxidizing prokaryotes in soils. Nature 442, 806–809.

Liu, J.Q., 1999. Volcanoes in China. Science Press of China, Beijing.

Loomis, S.E., Russell, J.M., Sinninghe Damsté, J.S., 2011. Distributions of branched GDGTs in soils and lake sediments from western Uganda: implications for a lacustrine paleothermometer. Org. Geochem. 42, 739–751.

Loomis, S.E., Russell, J.M., Ladd, B., Street-Perrott, F.A., Sinninghe Damsté, J.S., 2012. Calibration and application of the branched GDGT temperature proxy on East African lake sediments. Earth Planet. Sci. Lett. 357-358, 277–288.

Mingram, J., Schettlera, G., Nowaczyk, N., Luo, X., Lü, H., Liu, J., Negendank, J.F.W., 2004. The Huguang maar lake—a high-resolution record of palaeoenvironmental and palaeoclimatic changes over the last 78,000 years from South China. Quat. Int. 122, 85–107.

Naeher, S., Peterse, F., Smittenberg, R.H., Niemann, H., Zigah, P.K., Schubert, C.J., 2014. Sources of glycerol dialkyl glycerol tetraethers (GDGTs) in catchment soils, water column and sediments of Lake Rotsee (Switzerland) — implications for the application of GDGT-based proxies for lakes. Org. Geochem. 66, 164–173.

Pearson, E.J., Juggins, S., Talbot, H.M., Weckström, J., Rosén, P., Ryves, D.B., Roberts, S.J., Schmidt, R., 2011. A lacustrine GDGT-temperature calibration from the Scandinavian Arctic to Antarctic: renewed potential for the application of GDGT-paleothermometry in lakes. Geochim. Cosmochim. Acta 75, 6225–6238.

Peterse, F., van der Meer, J., Schouten, S., Weijers, J.W.H., Fierer, N., Jackson, R.B., Kim, J.-K., Sinninghe Damsté, J.S., 2012. Revised calibration of the MBT–CBT paleotemperature proxy based on branched tetraether membrane lipids in surface soils. Geochim. Cosmochim. Acta 96, 215–229.

Pilskaln, C.H., Johnson, T.C., 1991. Seasonal signals in Lake Malawi sediments. Limnol. Oceanogr. 36, 544–557.

Pitcher, A., Rychlik, N., Hopmans, E.C., Spieck, E., Rijpstra, W.I.C., Ossebaar, J., Schouten, S., Wagner, M., Sinninghe Damsté, J.S., 2010. Crenarchaeol dominates the membrane lipids of candidatus *Nitrososphaera gargensis*, a thermophilic group I.1b archaeon. ISME J. 4, 542–552.

Powers, L.A., Johnson, T.C., Werne, J.P., Castañeda, I.S., 2005. Large temperature variability in the southern African tropics since the Last Glacial Maximum. Geophys. Res. Lett. 32, L08706. http://dx.doi.org/10.1029/2004GL02014.

Powers, L.A., Werne, J.P., Vanderwoude, A.J., Sinninghe Damsté, J.S., Hopmans, E.C., Schouten, S., 2010. Applicability and calibration of the TEX_{86} paleothermometer in lakes. Org. Geochem. 41, 404–413.

Schouten, S., Hopmans, E.C., Schefuß, E., Sinninghe Damsté, J.S., 2002. Distributional variations in marine crenarchaeotal membrane lipids: a new organic proxy for reconstructing ancient sea water temperatures? Earth Planet. Sci. Lett. 204, 265–274.

Schouten, S., Huguet, C., Hopmans, E.C., Kienhuis, M.V.M., Sinninghe Damsté, J.S., 2007. Analytical methodology for TEX_{86} paleothermometry by high-performance liquid chromatography/atmospheric pressure chemical ionization-mass spectrometry. Anal. Chem. 79, 2940–2944.

Schouten, S., Hopmans, E.C., Sinninghe Damsté, J.S., 2013. The organic geochemistry of glycerol dialkyl glycerol tetraether lipids: a review. Org. Geochem. 54, 19–61.

Shultz, D., Calder, J.A., 1976. Organic carbon $^{13}C/^{12}C$ variations in estuarine sediments. Geochim. Cosmochim. Acta 40, 381–385.

Sinninghe Damsté, J.S., Schouten, S., Hopmans, E.C., van Duin, A.C.T., Geenevasen, J.A.J., 2002. Crenarchaeol: the characteristic core glycerol dibiphytanyl glycerol tetraether membrane lipid of cosmopolitan pelagic crenarchaeota. J. Lipid Res. 43, 1641–1651.

Sinninghe Damsté, J.S., Ossebaar, J., Abbas, B., Schouten, S., Verschuren, D., 2009. Fluxes and distribution of tetraether lipids in an equatorial African lake: constraints on the application of the TEX_{86} palaeothermometer and BIT index in lacustrine settings. Geochim. Cosmochim. Acta 73, 4232–4249.

Spang, A., Hatzenpichler, R., Brochier-Armanet, C., Rattei, T., Tischler, P., Spieck, E., Streit, W., Stahl, D.A., Wagner, M., Schleper, C., 2010. Distinct gene set in two different lineages of ammonia-oxidizing archaea supports the phylum Thaumarchaeota. Trends Microbiol. 18, 331–340.

Sun, Q., Chu, G., Liu, M., Xie, M., Li, S., Ling, Y., Wang, X., Shi, L., Jia, G., Lű, H., 2011. Distribution and temperature dependence of branched glycerol dialkyl glycerol tetraethers in recent lacustrine sediments from China and Nepal. J. Geophys. Res. 116, G01008. http://dx.doi.org/10.1029/2010JG001365.

Sun, C.H., Ren, F.M., Zhou, B., Gong, Z.Q., Zuo, J.Q., Guo, Y.J., 2012. Features and possible causes for the lower temperature in winter 2011/2012. Meteorol. Monogr. 38 (7), 884–889 (in Chinese with English abstract).

Tierney, J.E., Russell, J.M., 2009. Distributions of branched GDGTs in a tropical lake system: implications for lacustrine application of the MBT/CBT paleoproxy. Org. Geochem. 40, 1032–1036.

Tierney, J.E., Russell, J.M., Huang, Y., Sinninghe Damsté, J.S., Hopmans, E.C., Cohen, A.S., 2008. Northern hemisphere controls on tropical southeast African climate during the past 60,000 years. Science 322, 252–255.

Tierney, J.E., Mayes, M.T., Meyer, N., Johnson, C., Swarzenski, P.W., Cohen, A.S., Russell, J.M., 2010a. Late-twentieth-century warming in Lake Tanganyika unprecedented since AD 500. Nat. Geosci. 3, 422–425.

Tierney, J.E., Russell, J.M., Eggermont, H., Hopmans, E.C., Verschuren, D., Sinninghe Damsté, J.S., 2010b. Environmental controls on branched tetraether lipid distributions in tropical East African lake sediments. Geochim. Cosmochim. Acta 74, 4902–4918.

Walsh, E.M., Ingalls, A.E., Keil, R.G., 2008. Sources and transport of terrestrial organic matter in Vancouver Island fjords and the Vancouver–Washington Margin: a multiproxy approach using δ^{13}Corg, lignin phenols, and the ether lipid BIT index. Limnol. Oceanogr. 53, 1054–1063.

Wang, S.Y., Lu, H.Y., Liu, J.Q., Negendank, J.F.W., 2007. The early Holocene optimum inferred from a high-resolution pollen record of Huguangyan Maar Lake in southern China. Chin. Sci. Bull. 52, 2829–2836.

Wang, L., Lü, H.Y., Liu, J.Q., Gu, Z.Y., Mingram, J., Chu, G.Q., Li, J.J., Rioual, P., Negendank, J.F.W., Han, J.T., Liu, T.S., 2008. Diatom-based inference of variations in the strength of Asian winter monsoon winds between 17,500 and 6000 calendar years BP. J. Geophys. Res. Atmos. 113 (D21). http://dx.doi.org/10.1029/2008JD010145.

Wang, L., Li, J.J., Lü, H.Y., Gu, Z.Y., Rioual, P., Hao, Q.Z., Mackay, A.W., Jiang, W.Y., Cai, B.G., Xu, B., Han, J.T., Chu, G.Q., 2012. The East Asian winter monsoon over the last 15,000 years: its links to high-latitudes and tropical climate systems and complex correlation to the summer monsoon. Quat. Sci. Rev. 32, 131–142.

Weijers, J.W.H., Schefuβ, E., Schouten, S., Sinninghe Damsté, J.S., 2007a. Coupled thermal and hydrological evolution of tropical Africa over the last deglaciation. Science 315, 1701–1703.

Weijers, J.W.H., Schouten, S., Van Den Donker, J.C., Hopmans, E.C., Sinninghe Damsté, J.S., 2007b. Environmental controls on bacterial tetraether membrane lipid distribution in soils. Geochim. Cosmochim. Acta 71, 703–713.

Woltering, M., Johnson, T.C., Werne, J.P., Schouten, S., Sinninghe Damsté, J.S., 2011. Late Pleistocene temperature history of Southeast Africa: a TEX_{86} temperature record from Lake Malawi. Palaeogeogr. Palaeoclimatol. Palaeoecol. 303, 93–102.

Wu, X.D., Zhang, Z.H., Xu, X.M., Shen, J., 2012. Asian summer monsoonal variations during the Holocene revealed by Huguangyan maar lake sediment record. Palaeogeogr. Palaeoclimatol. Palaeoecol. 323-325, 13–21.

Yancheva, G., Nowaczyk, N.R., Mingram, J., Dulski, P., Schettler, G., Negendank, J.F.W., Liu, J.Q., Sigman, D.M., Peterson, L.C., Haug, G.H., 2007. Influence of the intertropical convergence zone on the East Asian monsoon. Nature 445, 74–77.

Zhang, C.X., Sun, S.L., Xie, S.Y., Xie, W.L., Zhan, D.L., 2008. The phytoplankton of the Huguangyan Maar Lake. Acta Hydrobiol. Sin. 32, 620–630 (in Chinese with English abstract).

Zheng, Z., Lei, Z., 1999. A 400,000 year record of vegetational and climatic changes from a volcanic basin, Leizhou Peninsula, southern China. Palaeogeogr. Palaeoclimatol. Palaeoecol. 145, 339–362.

Zhou, H.D., Hu, J.F., Spiro, B., Peng, P.A., Tang, J.H., 2014. Glycerol dialkyl glycerol tetraethers in surficial coastal and open marine sediments around China: indicators of sea surface temperature and effects of their sources. Palaeogeogr. Palaeoclimatol. Palaeoecol. 395, 114–121.

Zink, K.G., Vandergoes, M.J., Mangelsdorf, K., Dieffenbacher-Krall, A.C., Schwark, L., 2010. Application of bacterial glycerol dialkyl glycerol tetraethers (GDGTs) to develop modern and past temperature estimates from New Zealand lakes. Org. Geochem. 41, 1060–1066.